

# Improving The Radiometric Search of Anisotropic Stochastic Gravitational Wave Background with a Natural Set of Basis Functions

A Thesis

submitted to

Indian Institute of Science Education and Research Pune

in partial fulfillment of the requirements for the

BS-MS Dual Degree Programme

by

Pranjal Upadhyaya



Indian Institute of Science Education and Research Pune

Dr. Homi Bhabha Road,  
Pashan, Pune 411008, INDIA.

May, 2020

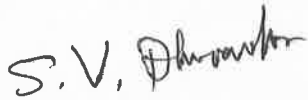
Supervisor: Sanjeev V. Dhurandhar

© Pranjal Upadhyaya 2020

All rights reserved

# Certificate

This is to certify that this dissertation entitled *Improving The Radiometric Analysis of Stochastic Gravitational Wave Background using a New Set of Basis Functions* towards the partial fulfilment of the BS-MS dual degree programme at the Indian Institute of Science Education and Research, Pune represents study/work carried out by Pranjal Upadhyaya at Indian Institute of Science Education and Research under the supervision of Sanjeev V. Dhurandhar, Emeritus Professor, Department of Physics, IUCAA, during the academic year 2019-2020.



Sanjeev V. Dhurandhar



Pranjal Upadhyaya

Committee:

Sanjeev V. Dhurandhar



Professor Suneeta Vardarajan

This thesis is dedicated to my parents

# Declaration

I hereby declare that the matter embodied in the report entitled *Improving The Radiometric Analysis of Stochastic Gravitational Wave Background using a New Set of Basis Functions*, is the result of the work carried out by me at the Department of Physics, IUCAA, Indian Institute of Science Education and Research, Pune, under the supervision of Sanjeev V. Dhurandhar and the same has not been submitted elsewhere for any other degree.



Sanjeev V. Dhurandhar



Pranjal Upadhyaya

# Acknowledgment

I would like to thank Professor Sanjeev V. Dhurandhar and Professor Shivaraj Kandhasamy for guiding me through this project and giving me an opportunity to work with them. Prof. Kandhasamy's expertise in coding really helped me out during the course of this project. I would also like to thank IISER Pune and IUCAA for providing me with their extensive library services that were instrumental in my research. I would also like to extend my thanks to my parents and my batchmates for their moral support during the course of this project.

# Abstract

The analysis of stochastic gravitational wave background involves the cross-correlation of signals detected by the two detectors at short time intervals augmented by a filter to optimize the signal to noise ratio. The rotation of Earth leads to a change in the baseline with respect to the signal coming from a particular direction in the sky which causes interference which is used to sample the Gravitational Wave Background. This however leads to a point spread function which means that the contribution from a single source spreads across the sky-sphere. The statistic that is obtained from this analysis shows that the contribution at each point is a weighted sum from the sources over the entire sky. If the sky is divided into  $n$  pixels, the weights form a  $n \times n$  matrix dubbed the beam pattern matrix. The power is now obtained by solving  $n$  linear algebraic equations in power. This process is called deconvolution. The aim of this project is to get a basis to represent the beam pattern matrix and do away with the need to deconvolve the map which is a cumbersome process. The basis being optimized to the problem might also provide some new insight into the problem.

# Contents

<b>Abstract</b>	<b>vii</b>
<b>1 Introduction</b>	<b>3</b>
<b>2 Statistic</b>	<b>6</b>
2.1 The Principle Behind the Cross-Correlation Statistic . . . . .	6
2.2 Cross-Correlation in the Frequency Domain . . . . .	8
2.3 Pixel Basis . . . . .	12
2.4 Dirty Map . . . . .	14
<b>3 Point Spread Function</b>	<b>16</b>
3.1 Stationary Phase Approximation . . . . .	16
3.2 SPA of the beam pattern matrix . . . . .	17
3.3 PSF . . . . .	20
3.4 Power Distribution . . . . .	22
<b>4 Groebner Basis and Stereographic Projection</b>	<b>25</b>
4.1 Basics of Algebraic Geometry . . . . .	25
4.2 Groebner Basis for Point Spread Function . . . . .	29



4.3	Stereographic Projection . . . . .	30
<b>5</b>	<b>Singular Value Decomposition</b>	<b>36</b>
5.1	Spherical Decomposition of Singular Vectors . . . . .	41
<b>6</b>	<b>An Approximate Basis</b>	<b>45</b>
<b>7</b>	<b>Conclusion and Future Possibilities</b>	<b>47</b>

# Preliminaries

**Basic Formulas:** The unit vectors in spherical polar coordinates:

$$\hat{\mathbf{r}} = (\sin \theta \cos \phi, \sin \theta \sin \phi, \cos \theta) \quad (1)$$

$$\hat{\mathbf{e}}_\theta = (\cos \theta \cos \phi, \cos \theta \sin \phi, -\sin \theta) \quad (2)$$

$$\hat{\mathbf{e}}_\phi = (-\sin \phi, \cos \phi, 0) \quad (3)$$

The polarization tensors  $e^+$  and  $e^\times$  are given by:

$$e^+ = e_\theta \otimes e_\theta - e_\phi \otimes e_\phi \quad (4)$$

$$e^\times = e_\theta \otimes e_\phi + e_\phi \otimes e_\theta \quad (5)$$

Consider a detector whose location is given by the latitude  $\frac{\pi}{2} - \theta$  and longitude  $\phi$ . If  $\psi$  denotes the angle the arm of the detector makes with the great circle running along its latitude location, then the detector arm locations assuming that the angle between the arms themselves is  $90^\circ$  is:

$$\mathbf{X} = (-\sin \phi \cos \psi - \cos \phi \cos \theta \sin \psi, \cos \phi \cos \psi - \sin \phi \cos \theta \sin \psi, \sin \theta \sin \psi) \quad (6)$$

$$\mathbf{Y} = (\sin \psi \sin \phi - \cos \phi \cos \theta \cos \psi, -\sin \psi \cos \phi - \sin \phi \cos \theta \cos \psi, \sin \theta \cos \psi) \quad (7)$$

Note that equation of the arm is given according to a basis that is rotating with Earth.

In order to get the vectors  $\mathbf{X}$  and  $\mathbf{Y}$  in a coordinate system that is fixed, we must multiply by the rotation matrix  $\mathbf{R}$ .

# Chapter 1

## Introduction

The advent of the gravitational wave detectors and the successful detection of colliding black hole and neutron star binaries has opened the channel for work on determining the large scale structures of the universe using gravitational wave astronomy. One of the leading push in this direction is to figure out the stochastic gravitational wave background. The stochastic gravitational wave background like the CMB can provide information about the evolution of large scale structures in the universe. It can have its origin either in cosmological sources or astrophysical. Since there does not exist a viable and testifiable cosmological model to account for any stochastic gravitational wave background, the source is more likely to be astrophysical like a region in the sky with a very large population of colliding binaries or other sources of gravitational waves. The virgo supercluster for example can be such a location. An important thing to consider here is that unlike the CMB, it is very difficult to determine the time of formation of this stochastic gravitational wave background owing to the nonlinearity of the Einstein's field equations and the lack of a parameter that can be associated to time, like the temperature in case of CMB. The space we are therefore working with is a quotient space i.e. we have no information about the distance of the source (unless known by some other method) only its direction.

The analysis of stochastic gravitational wave background requires the cross-correlation of input signal from two different detectors. The data is collected for a single sidereal day since a stochastic background will remain constant over short time intervals and the earth's location in the barycentric co-ordinates does not alter much during this time interval.

Consider a detector at location  $\mathbf{r}$  on the globe. The gravitational wave signal at this location from an area  $d\Omega$  on the sky sphere centred around  $\hat{\Omega}$  is;

$$dh_{\mu\nu}(t, \mathbf{r}) = \int_{-\infty}^{\infty} \tilde{h}_A(f, \hat{\Omega}) e_{\mu\nu}^A e^{2\pi i f(t + \hat{\Omega} \cdot \mathbf{r}/c)} df d\Omega \quad (1.1)$$

where  $\tilde{h}_A(f, \hat{\Omega})$  is the fourier transform of of the gravitational wave signal.

Since the search is for a stochastic background the contribution is taken from the entire sky sphere.

This implies;

$$h_{\mu\nu}(t, \mathbf{r}) = \int_{-\infty}^{\infty} df \int_{S^2} \tilde{h}_A(f, \hat{\Omega}) e_{\mu\nu}^A e^{2\pi i f(t + \hat{\Omega} \cdot \mathbf{r}/c)} d\Omega \quad (1.2)$$

is the gravitational wave signal from the entire sky sphere at the detector location  $\mathbf{r}$ .

For a stochastic background the signal from different directions must be uncorrelated. There should also be no correlation between signals arriving at different frequencies.

Mathematically this condition is represented by the equation;

$$\langle \tilde{h}_A^*(f, \hat{\Omega}) \tilde{h}_A(f', \hat{\Omega}') \rangle = \delta(f - f') \delta^2(\hat{\Omega} - \hat{\Omega}') P_A(\hat{\Omega}) H(f) \quad (1.3)$$

The mean described above is a statistical mean and is a quantity that will be used frequently through this analysis.

$P_A(\hat{\Omega})$  is the power in polarization A from the direction  $\hat{\Omega}$  on the sky-sphere.  $H(f)$  is the spectral power density i.e.  $H(f)$  gives the distribution of power in the gravitational wave signal in the frequency domain. The signal detected by the detector I at time t is given by the gravitational wave strain function  $h_I(t)$ .

This function is given by the formula;

$$h_I(t) = d_I^{\mu\nu}(t) h_{\mu\nu}(t, \mathbf{r}_I) \quad (1.4)$$

where  $d_I^{\mu\nu}$  is the detector tensor for detector I and given by the equation

$$d^{\mu\nu} = \frac{1}{2}(X^\mu X^\nu - Y^\mu Y^\nu) \quad (1.5)$$

where  $\hat{X}$  and  $\hat{Y}$  are the normal vectors running along the length of the detector arms.

Expanding equation (1.4) using equation (1.2) and (1.5);

$$h_I(t) = \int_{-\infty}^{\infty} df \int_{S^2} h_A(f, \hat{\Omega}) e_{\mu\nu}^A(\hat{\Omega}) d_I^{\mu\nu}(t) e^{2\pi i f(t + \hat{\Omega} \cdot \mathbf{r}/c)} d\Omega \quad (1.6)$$

Denoting  $F_I^A(\hat{\Omega}, t) = e_{\mu\nu}^A(\hat{\Omega}) d_I^{\mu\nu}(t)$ .

It is to be noted that the output from the detector also contains noise and hence the output signal for the detector I at time t is given by;

$$s_I(t) = h_I(t) + n_I(t)$$

In order to sample out the signal from the noise, data from two different detectors is cross-correlated with a time delay which is equal to the travel time between the two detectors.

# Chapter 2

## Statistic

### 2.1 The Principle Behind the Cross-Correlation Statistic

Consider two detectors located at  $\mathbf{r}_1(t)$  and  $\mathbf{r}_2(t)$  on the globe. Consider a gravitational wave signal coming from a direction  $\hat{\Omega}$  on the sky sphere. Note that the signal is approaching radially assuming large distances between the source and Earth. Because of the separation between the detectors at any given time  $t$  there is a time delay between the signal detected by the two detectors. If  $\Delta\mathbf{r}(t)$  denotes the vector joining detector 1 and detector 2, the additional distance the gravitational wave signal has to travel between the detectors is given by  $\Delta\mathbf{r} \cdot \hat{\Omega}$ . Thus the time delay between the signal is given by  $\tau = \frac{\Delta\mathbf{r} \cdot \hat{\Omega}}{c}$  where  $c$  is the speed of light.

Now if the signal from the two detectors is cross-correlated with time delay  $\tau$ , the signals will interfere constructively. For any other time delay, the interference will be destructive. Another way to think about it is that if the signal approaches from a direction other than  $\hat{\Omega}$  say  $\hat{\Omega}'$ , the signals when cross correlated with time delay  $\tau$  will interfere destructively because the time delay  $\tau'$  for the sky direction  $\hat{\Omega}'$  will be different from  $\tau$ .

Because of Earth's rotation  $\tau$  also changes and hence for a fixed time delay the direction from which the incoming signals interfere constructively changes with time. Thus the two

detectors make a baseline that changes with time and can be used to sample the sky sphere.

Numerically the cross-correlation is performed at time intervals of a finite width. In order to find an appropriate time interval, lower and upper bounds for this interval must be calculated. The upper bound can be any time interval over which the angular change in the baseline is small enough to be ignored. But for accuracy in the numerical calculation the smallest of these upper bounds is chosen. The lower bound comes from the time taken by the gravitational wave to travel between the two detectors  $t_d$ . This time interval is calculated by assuming light travel along the length of the detector. If the time interval is chosen to be smaller than  $t_d$ , the signal will be incoherent since we will be cross-correlating signals belonging to different section of the incoming gravitational wave with no overlap.

The way to achieve this cross-correlation is by introducing a direction dependent filter  $Q(t, \hat{\Omega}, t', t'')$  which cross-correlates the signal from detector i at time  $t'$  with that of detector j at  $t''$  with time delay t. If  $s_I(t)$  denotes the output from detector I. Then the quantity;

$$\Delta S(t, \hat{\Omega}) = \int_{t-\frac{\Delta t}{2}}^{t+\frac{\Delta t}{2}} dt' \int_{t-\frac{\Delta t}{2}}^{t+\frac{\Delta t}{2}} dt'' s_1(t') s_2(t'') Q(t, \hat{\Omega}, t', t'') \quad (2.1)$$

samples the signal from direction  $\hat{\Omega}$  with time delay t.

The time parameter t in the filter takes care of the baseline's rotation and hence the final statistic is obtained by integrating over the time parameter t in the directional filter;

$$S(\hat{\Omega}) = \int dt \Delta S(t, \hat{\Omega}) \quad (2.2)$$

Now any useful statistic in signal detection must maximize the signal to noise ratio. For  $S(\hat{\Omega})$ , this can be achieved by adding weights to the time sections such that the interval in which the signal interferes constructively is enhanced compared to the sections where destructive interference take place.

The statistic is therefore given by;

$$S(\hat{\Omega}) = \sum_{k=1}^n w_k(\hat{\Omega}) \Delta S(t_k, \hat{\Omega}) \quad (2.3)$$



where  $w_k$  are the said weights.

## 2.2 Cross-Correlation in the Frequency Domain

In order to further the analysis we move from time domain to frequency domain since we have a spectral power density and the gravitational wave strain which are both frequency dependent. Note however that since the statistic is divided into short time intervals, when the fourier transform is taken, we simply cannot take the fourier transform for time stretching across the entire day. Just like the statistic  $\Delta S(t, \hat{\Omega})$ , the time period over which the fourier transform is taken is divided into short intervals  $\Delta t$ .

Thus the Short Fourier Transform(SFT) for a quantity  $s(t')$  on a time interval  $\Delta t$  centred around  $t$  is given by the equation;

$$s(t; f) = \int_{t-\Delta\frac{t}{2}}^{t+\Delta\frac{t}{2}} dt' s(t') e^{-2\pi i f t'} \quad (2.4)$$

Thus the SFT of the detector strain function  $h_I(t)$  is given by

$$h_I(t; f) = \int_{t-\Delta\frac{t}{2}}^{t+\Delta\frac{t}{2}} dt' \int_{-\infty}^{\infty} df' \int_{S^2} d\Omega h_A(f', \hat{\Omega}) e_{\mu\nu}^A(\hat{\Omega}) d_I^{\mu\nu}(t') e^{2\pi i f'(t'+\hat{\Omega}\cdot\mathbf{r}/c)} e^{-2\pi i f t'} \quad (2.5)$$

Consider the integral;

$$\int_{t-\Delta\frac{t}{2}}^{t+\Delta\frac{t}{2}} dt' e^{-2\pi i f t'} = e^{-2\pi i f t} \frac{\sin \pi f \Delta t}{\pi f} \quad (2.6)$$

Defining the short time delta function  $\delta_{\Delta t}(f) = \frac{\sin \pi f \Delta t}{\pi f}$ . Note that in the limit of large  $\Delta t$ , the short time delta function goes to our normal Dirac delta.

Using this result to integrate over  $t'$  in equation (1.11) under the assumption that  $d_I^{\mu\nu}(t)$

is constant on the time interval  $\Delta t$  centred at time  $t$ ;

$$h_I(t; f) = \int_{-\infty}^{\infty} df' \int_{S^2} d\Omega h_A(f', \hat{\Omega}) e_{\mu\nu}^A(\hat{\Omega}) d_I^{\mu\nu}(t) e^{(2\pi i(f'-f)t' + 2\pi i f' \hat{\Omega} \cdot \mathbf{r}/c)} \quad (2.7)$$

In order to get the SNR ratio the mean and variance of  $\Delta S(t, \hat{\Omega})$  must be calculated

Now the mean of  $\Delta S(t, \hat{\Omega})$  is defined as;

$$\langle \Delta S(t, \hat{\Omega}) \rangle = \int dt' \int dt'' \langle s_1(t') s_2(t'') \rangle Q(t, \hat{\Omega}, t', t'') \quad (2.8)$$

Considering the quantity that inside the integral is being averaged over.

$$\langle \tilde{s}_1(t') s_2(t'') \rangle = \langle \tilde{h}_1(t') h_2(t'') \rangle + \langle \tilde{h}_1(t') n_2(t'') \rangle + \langle \tilde{n}_1(t') h_2(t'') \rangle + \langle \tilde{n}_1(t') n_2(t'') \rangle \quad (2.9)$$

The noise in detector I is uncorrelated to the detector strain at detector I as well as the detector strain at another detector J. The noise in a detector is also uncorrelated to the noise in another detector given the detectors are far away from each other. The reason for this is the noise has its origin in the conditions local to the detector while the strain originates from non local sources.

This implies  $\langle s_1(t') s_2(t'') \rangle = \langle h_1(t') h_2(t'') \rangle$ .

Calculating this average by moving into the frequency domain;

$$\begin{aligned} \langle \tilde{h}_1^*(t, f) h_2(t, f') \rangle &= \int_{t-\Delta\frac{t}{2}}^{t+\Delta\frac{t}{2}} dt' \int_{t-\Delta\frac{t}{2}}^{t+\Delta\frac{t}{2}} dt'' \int_{-\infty}^{\infty} df'' \int_{-\infty}^{\infty} df''' \int_{S^2} d\Omega \int_{S^2} d\Omega' \langle \tilde{h}_A^*(f'', \hat{\Omega}) \tilde{h}_A(f''', \hat{\Omega}') \rangle \\ &\quad e_{\mu\nu}^A(\hat{\Omega}) d_1^{\mu\nu}(t) e_{\alpha\beta}^A(\hat{\Omega}') d_2^{\alpha\beta}(t) e^{(2\pi i(f-f'')t' - 2\pi i f'' \hat{\Omega} \cdot \mathbf{r}_1/c)} e^{(2\pi i(f'''-f')t'' + 2\pi i f''' \hat{\Omega}' \cdot \mathbf{r}_2/c)} \quad (2.10) \end{aligned}$$

Carrying out the integration over  $t'$ ,  $t''$ ,  $\Omega'$  and  $f'''$  making use of equation (1.3);

$$\langle \tilde{h}_1^*(t, f) h_2(t, f') \rangle = \int_{-\infty}^{\infty} df'' H(f'') \gamma(t, f''; \Delta\Omega, dP_A) \delta_{\Delta t}(f'' - f) \delta_{\Delta t}(f'' - f') \quad (2.11)$$

where;

$$\gamma(t, f''; \Delta\Omega, dP_A) = \int_{\Delta\Omega=S^2} d\Omega [F_1^+(\hat{\Omega}, t)F_2^+(\hat{\Omega}, t)P_+(\hat{\Omega}) + F_1^\times(\hat{\Omega}, t)F_2^\times(\hat{\Omega}, t)P_\times(\hat{\Omega})] e^{2\pi i f \hat{\Omega} \cdot \Delta \mathbf{r}/c} \quad (2.12)$$

The quantity  $\gamma(t, f''; \Delta\Omega, dP_A)$  is called the overlap reduction function. It is this term that carries the phase according to which the interference takes place. Notice the parameters of the reduction function involves the measure  $dP_A(\hat{\Omega})$ .

Another important quantity to calculate is the noise power spectral density as it will contribute to the variance of the statistic. For a time segment centered at  $t$ , this quantity is given by using the following equation;

$$\langle n_I(t') n_I(t'') \rangle = \frac{1}{2} \int_{-\infty}^{\infty} df P_I(t; |f|) e^{2\pi i f (t'' - t')} \quad (2.13)$$

$P_I(t; |f|)$  is the one sided noise power spectral density.

Now we have all the quantities required to calculate the statistic. The only issue is to figure out the weight's  $w_k$  and the directional filter  $Q(t, \hat{\Omega}; t', t'')$ . They are calculated by getting the equation for the SNR for the statistic which is  $\rho_S \sigma_S$  where,

$$\rho_S = \sum_{k=1}^n w_k \langle \Delta S(t_k, \hat{\Omega}) \rangle \quad (2.14)$$

is the average of the statistic, and

$$\sigma_S^2 = \langle (\Delta S(t_k, \hat{\Omega}))^2 \rangle - (\langle \Delta S(t_k, \hat{\Omega}) \rangle)^2 \quad (2.15)$$

is the the standard deviation of  $\xi(\hat{\Omega})$  The SNR is now maximized first with respect to  $w_k$  and with respect to the directional filter  $Q(t, \hat{\Omega}; t', t'')$ . (For details see [1].) After following through with this process, the obtained statistic is;

$$S(\hat{\Omega}) = \int_{S^2} B^+(\hat{\Omega}, \hat{\Omega}') P_+ + B^\times(\hat{\Omega}, \hat{\Omega}') P_\times d\Omega' \quad (2.16)$$

where the beam pattern function is given by:

$$B^A(\widehat{\Omega}, \widehat{\Omega}') = \Lambda(\widehat{\Omega}) \int \int_{-\infty}^{\infty} \frac{H(f)H'(f)}{P_1(t, |f|)P_2(t, |f|)} F_1^A(\widehat{\Omega}', t) F_2^A(\widehat{\Omega}', t) \Gamma(\widehat{\Omega}, t) e^{-2\pi i f(\widehat{\Omega} - \widehat{\Omega}') \cdot \Delta r(t)} df dt \quad (2.17)$$

The quantity  $\Lambda$  is a normalization factor.

$$F_I^A(\widehat{\Omega}, t) = e_{\mu\nu}^A(\widehat{\Omega}) d^{\mu\nu}(t) \quad (2.18)$$

$$\Gamma(\widehat{\Omega}, t) = F_I^+(\widehat{\Omega}, t) + F_I^\times(\widehat{\Omega}, t) \quad (2.19)$$

In order to ease further analysis the background is taken to be unpolarized i.e  $P_\times(\widehat{\Omega}) = P_+(\widehat{\Omega})$ . The noise is also taken to be white. Note that  $H(f)$  is not necessarily known for it depends on the source. This quantity will also be set to unity. This is an assumption we will be working with from here on out. A thing to be added here is that if the background is indeed polarized, the statistic we are deriving will not be able to determine the power in each polarization from each direction, since the number of independent power sources will be twice the number of points sampled from the skt sphere. For such an analysis, some sort of a polarization filter will have to be introduced.

Thus the final equation of interest is

$$B(\widehat{\Omega}, \widehat{\Omega}') = \Lambda(\widehat{\Omega}) \int \int_{-\infty}^{\infty} \frac{H(f)H'(f)}{P_1(t, |f|)P_2(t, |f|)} \Gamma(\widehat{\Omega}', t) \Gamma(\widehat{\Omega}, t) e^{-2\pi i f(\widehat{\Omega} - \widehat{\Omega}') \cdot \Delta r(t)} df dt \quad (2.20)$$

and

$$S(\widehat{\Omega}) = \int_{S^2} B(\widehat{\Omega}, \widehat{\Omega}') P(\widehat{\Omega}') d\Omega' \quad (2.21)$$

Let  $B_{ij}$  denote the element of the beam pattern matrix which is in  $i^{th}$  row and  $j^{th}$  column. This entry denotes the power registered in the direction  $\Omega_i$  because of a source with unit

power in the direction  $\Omega_j$ . Thus the  $j^{th}$  column gives the spread of a source of unit power in the direction  $\Omega_j$ . Note that the beam pattern matrix described earlier is a symmetric matrix if the normalization is made direction independent. Thus the beam matrix describes the weighted power spread for a source in the sky and in reciprocity it is these point spreads that construct statistic.

## 2.3 Pixel Basis

The sampling of the sky sphere by any detector pair does not occur with infinite accuracy because of physical constraints like the sensitivity of the detectors. The accuracy of the detection apart from the effects of noise is determined by the operational bandwidth of the detectors. Though in the equations derived, integration over frequency is taken from  $-\infty$  to  $\infty$  in reality there is an upper and a lower bound between which the frequency is integrated. The second parameter that determines the accuracy is the length of the baseline. Consider the bandwidth  $\Delta f$  that is detectable by the detector pairs under consideration. The corresponding wavelength of the gravitational wave signal is  $\lambda = \frac{c}{\Delta f}$ . Thus the angular width detected is  $\Delta\Omega = \frac{\lambda}{d}$  where  $d$  is the distance between the detector pairs. Since we are working in the pixel basis right now, the maximum number of pixels that can be sampled is given by  $n = \frac{4\pi}{\Delta\Omega^2}$ . (the  $4\pi$  is the solid angle of the entire sphere) Thus for the pair of LIGO detectors where  $d=3000$  km and  $\Delta f \sim 1000$ kHz,  $n_o \simeq 1200$ . Notice that in the limit of the bandwidth approaching  $\infty$ , the resolution and the number of pixels go to  $\infty$ . The numerical analysis therefore involves patches of the sky sphere instead of single points. Now the power from direction  $\hat{\Omega}$  is therefore taken to be spread over the patch. This allows us to define the measure  $dP_A(\hat{\Omega}) = P_A(\hat{\Omega})d\Omega$ .

So for an unpolarized stochastic background,  $S(\hat{\Omega}) = \int dP(\hat{\Omega}')B(\hat{\Omega}, \hat{\Omega}')$ . Now going from integration to sum,

$$S(\hat{\Omega}) = \sum_{\hat{\Omega}'} \Delta P(\hat{\Omega}')B(\hat{\Omega}, \hat{\Omega}'). \quad (2.22)$$

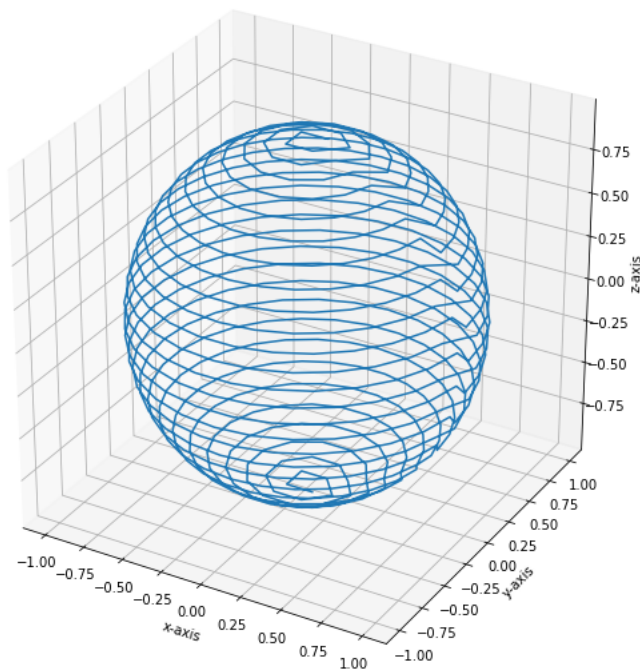
where  $\Delta P(\hat{\Omega}')$  is the power spread over the sky patch  $\hat{\Omega}'$ . But this quantity is  $P(\hat{\Omega}')$ . Hence;

$$S(\hat{\Omega}) = \sum_{\hat{\Omega}'} P(\hat{\Omega}')B(\hat{\Omega}, \hat{\Omega}'). \quad (2.23)$$

The most natural way to plot the above equation is through the use of the pixel basis. A pixel basis is set by dividing the entire sky sphere into pixels of equal area. There are multiple ways to achieve this. The pixelization scheme used in this thesis is an isolatitude equal area pixelization. The way it works is that the pixels are divided into groups such that, pixels belonging to the same group have the same latitude ( $\theta$ ) hence, it is called isolatitude pixelization. The reason to choose this particular scheme is that numerical integration using an isolatitude basis is much faster compared to pixelization schemes that are not isolatitudinal. In the  $(\theta, \phi)$  basis each pixel is described by the point at the centre of the pixel. The pixels are identified by a number called their index running from 0 to n-1 where n is the number of pixels. The numbering can be achieved in different ways. The one followed in this thesis is achieved in the following way

The pixel with index 0 is the one closest to the northpole and with  $\phi = 0$ . Going clockwise the pixel directly to the right is numbered 1. This continues until the pixel directly to the left of pixel 0 is reached. Then move down directly below pixel 0 and start the entire process again.

The figure below shows the sequence in which this is achieved;



Unless otherwise mentioned whenever pixelization is used the number of pixels is kept 588.

Equation number (2.29) can now be reformulated as a matrix equation. Let  $S(\widehat{\Omega}_i)$  be denoted by  $S_i$ ,  $P(\widehat{\Omega}_i)$  by  $P_i$  and  $B(\widehat{\Omega}_i, \widehat{\Omega}_j)$  by  $B_{ij}$ .

Denoting  $\mathbf{P} = \{P_1, P_2, \dots, P_n\}$ ,  $\mathbf{S} = \{S_1, S_2, \dots, S_n\}$  and describing a matrix  $\mathbf{B}$ . The element in the  $i^{th}$  row and  $j^{th}$  column of  $\mathbf{B}$  is given by  $B_{ij}$ .

Thus we have the equation;

$$\mathbf{S} = \mathbf{B} \cdot \mathbf{P} \tag{2.24}$$

## 2.4 Dirty Map

Plotting  $\mathbf{P}$  on the sky sphere the map obtained is the true map of the stochastic gravitational wave background. What we get however as a plot of the sky after the cross-correlation is  $\mathbf{S}$  which is a linear combination of the elements of the true sky map weighted by the elements of the beam pattern matrix.

Note that the beam pattern matrix described earlier is a symmetric matrix if the normalization is made direction independent. Thus the beam matrix is constructed by these structures. This map of the sky is called the sky sphere. The task we now have is to obtain the information about the true stochastic background. The beam pattern matrix is symmetric except for the normalization  $\Lambda(\widehat{\Omega})$  which can be set to unity.

Consider a scenario where there is a single source of power in the sky say at the location occupying pixel  $i$  (remember the pixels are marked by numbers). The resulting output is the first column of the beam pattern matrix, i.e. the source power has been spread over the entire sky sphere though with different weights. Thus we are dealing here with a point spread function. An analytical derivation of the shape and the weight at each point of the spread will be derived in the next section.

The problem at hand is therefore to get the true sky map from the dirty map. The most

straight forward way is to calculate the inverse of  $\mathbf{B}$  resulting in the equation;

$$\mathbf{B}^{-1} \cdot \mathbf{S} = \mathbf{P} \quad (2.25)$$

Though calculating the inverse of large matrices is both time and power consuming and is difficult for large matrices. For example, for the LIGO pair of detectors with bandwidth a few kilohertz, and the distance between them around 3000 kms, the minimum number of pixels required is around 1200 and in order to do away with discrepancies, the sky sphere is often oversampled. It is computationally extensive to handle such a large matrix. The method that is generally employed to deal with this situation is to use computer algorithms to solve the algebraic equations of the form  $S_i = \sum_{k=1}^n B_{ik} P_k$ . This procedure of numerically obtaining the true sky map from the dirty map is called deconvolution.

The idea of a basis for the dirty map and how it might do away with the highly involved deconvolution procedures using computer algorithms is described below:

Let  $\mathbf{b}_i$  denote the  $i^{th}$  column of  $\mathbf{B}$ . A basis  $\{\mathbf{v}_1, \mathbf{v}_2, \mathbf{v}_3, \dots, \mathbf{v}_n\}$  for the beam pattern matrix is the set of vectors that construct the  $b_i$ 's. Let  $\alpha_i^j$  denote the vector dot product  $\mathbf{v}_j^T \cdot \mathbf{b}_i$ . Thus  $\mathbf{b}_i$  can be written as;

$$\mathbf{b}_i = \sum_{k=1}^n \alpha_i^k \mathbf{v}_k \quad (2.26)$$

Then the vector dot product  $\mathbf{v}_j^T \cdot \mathbf{S}$  gives;

$$\sum_{k=1}^n \alpha_i^k P_k \quad (2.27)$$

A good basis will be such that the number of non-zero  $\alpha$ 's in the above equation is small enough to ease the calculation. Getting a good basis does more than just ease the calculation. It can also give a deeper insight into the problem.



# Chapter 3

## Point Spread Function

### 3.1 Stationary Phase Approximation

Consider an integral of the form  $\int_{t_l}^{t_u} f(t)g(t) dt$ , where both  $f(t)$  and  $g(t)$  are functions periodic in  $t$ . Consider that  $g(t)$  has a time period much smaller than  $f(t)$ . Consider a time interval  $2\Delta t$  is chosen centred around  $t$  such that the variation in  $f(t)$  is very small but  $g(t)$  varies significantly owing to its small time period. Then the sum

$$\int_{t-\Delta t}^{t+\Delta t} f(t)g(t) dt \simeq f(t) \int_{t-\Delta t}^{t+\Delta t} g(t) dt$$

If  $2\Delta t$  is of the same order of magnitude as the time period of  $g(t)$ , then the sum is 0 unless there is a critical point in the interval i.e. there exists a value  $t_o$  in the interval  $[t - \Delta t, t + \Delta t]$  such that  $\frac{dg(t)}{dt} = 0$ . If there indeed is a critical point in the interval the sum gives  $f(t_o)g(t_o)$ . This is the central idea behind stationary phase approximation.

Now consider an integral of the form;

$$\int_{t_l}^{t_u} f(t)e^{ig(t)} dt \tag{3.1}$$

Let  $t_o$  denote the critical point of  $g(t)$ . Taylor expanding  $g(t)$  around  $t_o$ ;

$$g(t) = g(t_o) + (t - t_o) \frac{dg(t_o)}{dt} + \frac{1}{2}(t - t_o)^2 \frac{d^2g(t_o)}{dt^2} + \dots \quad (3.2)$$

Since  $t_o$  is a critical point, the first order derivative of  $g(t)$  at  $t_o$  is zero.

Hence the integral (2.1) becomes;

$$f(t_o) e^{ig(t_o)} \int_{t_l}^{t_u} \exp\left(\frac{i}{2} \frac{d^2g(t_o)}{dt^2} (t - t_o)^2\right) dt \quad (3.3)$$

which is solved using contour integration.

## 3.2 SPA of the beam pattern matrix

The equation for the beam pattern matrix (1.8) has integral over both time and frequency and since the exponential term depends on both these parameters therefore SPA with respect to both frequency and time is carried out.

Let  $T(t)$  and  $F(f)$  denote functions depending only on time and frequency respectively. If  $t_o$  and  $f_o$  are the critical points respectively then Taylor expansion of the product  $T(t)F(f)$  upto second order has the form;

$$T(t)F(f) = T(t_o)F(f_o) + \frac{1}{2} \left( F(f_o)(t - t_o)^2 \frac{d^2T(t_o)}{dt^2} + T(t_o)(f - f_o)^2 \frac{d^2F(f_o)}{df^2} \right) \quad (3.4)$$

Replacing  $F(f)$  by  $f$  and  $T(t)$  by  $\Delta\Omega \cdot \Delta\mathbf{r}$  and setting the first order derivative to zero, the conditions for the stationary points are:

$$\Delta\Omega \cdot \Delta\mathbf{r}(t) = 0 \quad (3.5)$$

$$\Delta\Omega \cdot \Delta\dot{\mathbf{r}}(t) = 0 \quad (3.6)$$

Using the property of curl that;

$$\mathbf{A} \times (\mathbf{B} \times \mathbf{C}) = \mathbf{B}(\mathbf{A} \cdot \mathbf{C}) - \mathbf{C}(\mathbf{A} \cdot \mathbf{B}) \quad (3.7)$$

combined with equations (3.6) and (3.7);

$$\Delta\Omega(t) \times (\Delta\mathbf{r} \times \Delta\dot{\mathbf{r}}) = 0 \quad (3.8)$$

which implies that  $\Delta\Omega(t)$ ,  $\Delta\mathbf{r}$ , and  $\Delta\dot{\mathbf{r}}$  form an orthogonal triad.

Now using the fact  $\Delta\Omega(t) = \widehat{\Omega}(t) - \widehat{\Omega}_o$  and that both  $\widehat{\Omega}(t)$  and  $\widehat{\Omega}_o$  have unit norm;

$$\Delta\Omega^2 = -2\Delta\Omega \cdot \widehat{\Omega}_o \quad (3.9)$$

Defining the unit vector parallel to the baseline as;

$$\widehat{\mathbf{n}}_{cone}(t) = \frac{\Delta\mathbf{r} \times \Delta\dot{\mathbf{r}}}{|\Delta\mathbf{r} \times \Delta\dot{\mathbf{r}}|} \quad (3.10)$$

Since  $\Delta\Omega(t)$  is parallel to  $\widehat{\mathbf{n}}_{cone}(t)$ , therefore equation (3.1) becomes;

$$\Delta\Omega = -2\widehat{\mathbf{n}}_{cone} \cdot \widehat{\Omega}_o \quad (3.11)$$

$$\widehat{\Omega}(t) = \widehat{\Omega}_o - 2(\widehat{\mathbf{n}}_{cone} \cdot \widehat{\Omega}_o)\widehat{\mathbf{n}}_{cone} \quad (3.12)$$

### 3.2.1 Cone angle

Let  $\mathbf{r}_1(t) = R(\sin \theta_1 \cos \phi_1 \cos wt - \sin \theta_1 \sin \phi_1 \sin wt, \sin \theta_1 \cos \phi_1 \sin wt + \sin \theta_1 \sin \phi_1 \cos wt, \cos \theta_1)$  and  $\mathbf{r}_2 = R(\sin \theta_2 \cos \phi_2 \cos wt - \sin \theta_2 \sin \phi_2 \sin wt, \sin \theta_2 \cos \phi_2 \sin wt + \sin \theta_2 \sin \phi_2 \cos wt, \cos \theta_2)$  denote the position of two detectors where R is the radius of the Earth. The vector joining

the two detectors is given by

$$\begin{aligned} \Delta \mathbf{r} = R & ((\sin \theta_1 \cos \phi_1 - \sin \theta_2 \cos \phi_2) \cos wt - (\sin \theta_1 \sin \phi_1 - \sin \theta_2 \sin \phi_2) \sin wt, \\ & (\sin \theta_1 \cos \phi_1 - \sin \theta_2 \cos \phi_2) \sin wt + (\sin \theta_1 \sin \phi_1 - \sin \theta_2 \sin \phi_2) \cos wt, \cos \theta_1 - \cos \theta_2) \end{aligned} \quad (3.13)$$

If the detectors are not at the same latitude, the vector  $\Delta \mathbf{r}$  makes an angle  $\Theta$  with the z-axis. As the earth rotates, the vector  $\Delta \mathbf{r}$  also rotates while maintaining the angle  $\Theta$  with the z-axis. Thus, after one complete rotation around the globe the vector,  $\Delta \mathbf{r}$  carves out a cone centred at the origin and the z-axis as its axis of symmetry. The shape of the PSF is therefore given by the intersection of this cone with the sky sphere with the centre on the cone located at the source location. In the next section these shapes will be studied.

The distance between the detectors is constant and is given by:

$$\Delta r = R \sqrt{2[1 - \cos \theta_1 \cos \theta_2 - \sin \theta_1 \sin \theta_2 (\cos \phi_1 - \cos \phi_2)]} \quad (3.14)$$

Now the cone angle  $\Theta$  is defined as  $\cos \Theta = \hat{\mathbf{z}} \cdot \Delta \hat{\mathbf{r}}$ . Using equation (3.4) and (3.5), the cone angle is given by the equation;

$$\cos \Theta = \frac{\cos \theta_1 - \cos \theta_2}{\sqrt{2[1 - \cos \theta_1 \cos \theta_2 - \sin \theta_1 \sin \theta_2 (\cos \phi_1 - \cos \phi_2)]}} \quad (3.15)$$

Using the above equation combined with equation (3.14);

$$\Delta \mathbf{r} = \Delta r (\sin \Theta \cos (\Phi + wt), \sin \Theta \sin (\Phi + wt), \cos \Theta) \quad (3.16)$$

where,

$$\cos \Phi = \frac{\sin \theta_1 \cos \phi_1 - \sin \theta_2 \cos \phi_2}{\sqrt{\sin^2 \theta_1 + \sin^2 \theta_2 - 2 \sin \theta_1 \sin \theta_2 \cos \phi_1 - \phi_2}} \quad (3.17)$$

is the angle between the vector  $\Delta \mathbf{r}$  and the x-axis.

Because of rotational symmetry, without any loss of generality, the x-axis can be chosen

to be along  $\Delta\mathbf{r}$ . This implies;

$$\Delta\mathbf{r} = \Delta r(\sin \Theta \cos wt, \sin \Theta \sin wt, \cos \Theta) \quad (3.18)$$

### 3.3 PSF

Using equation (3.10), (3.12) and (3.18)  $\widehat{\Omega}(t)$  can now be calculated. Denoting  $\widehat{\Omega}(t) = (x(t), y(t), z(t))$  the following equations are obtained

$$x(t) = \sin \theta \cos \phi - 2 \cos^2 \Theta \sin \theta \cos(\phi - wt) \cos wt + \sin 2\Theta \cos \theta \cos wt \quad (3.19)$$

$$y(t) = \sin \theta \sin \phi - 2 \cos^2 \Theta \sin \theta \cos(\phi - wt) \sin wt + \sin 2\Theta \cos \theta \sin wt \quad (3.20)$$

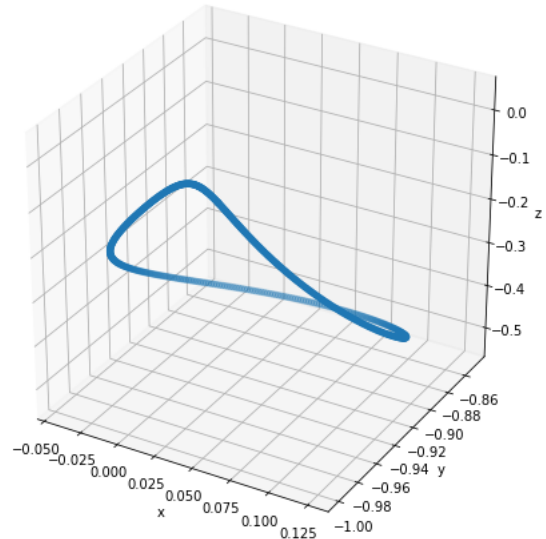
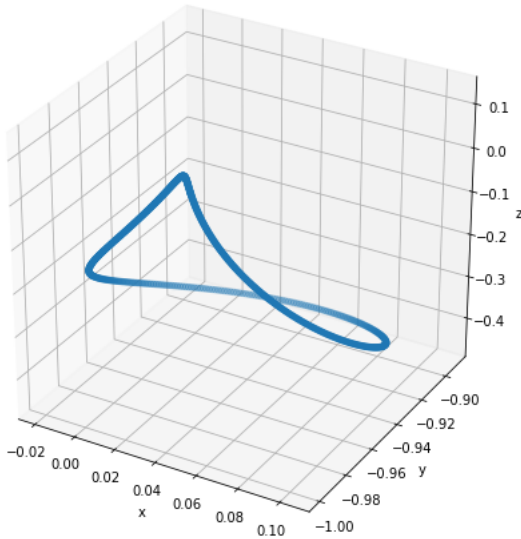
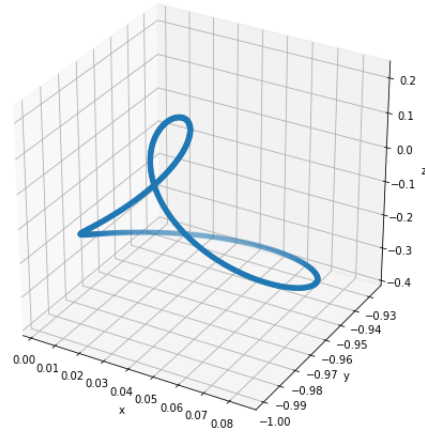
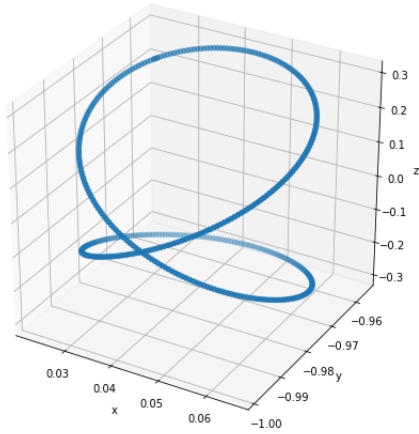
$$z(t) = \cos 2\Theta \cos \theta + \sin 2\Theta \sin \theta \cos(\phi - wt) \quad (3.21)$$

The above equations give the spread of a source at the location  $(\theta, \phi)$  on the sky sphere.

Notice the time dependence that has propped up even though the statistic was obtained by integrating over time. The reason for this is the way the statistic was defined by cross-correlating signal from a particular direction on the sky-sphere at different time delays. The signals interfere constructively when the time delay matches the travel time between the detectors. Since the time delay is changed, the section of the sky contributing constructively to the signal is also changing. Thus different sections of the sky contribute to a point on the dirty map at different times.

These structures are not bases as they are not linearly independent. In fact the space that we are working with is overcomplete.

The figure below shows the shape of the spread function for different values of  $\theta$ . These structures are symmetric in  $\phi$  as expected.



From left to right the latitude of the source goes from  $0^\circ$  to  $15^\circ$ .

As can be seen from the plot, for a source at the equator the spread is in the form of a figure of 8 which changes into a tear drop shape as the source is moved along the longitude to higher latitudes.

An interesting calculation that can be done is to figure out the time when a source in the sky at location  $(\theta, \phi)$  contributes at its own location in the dirty map. This can be done by simply putting in the source location in place of  $x(t), y(t)$  and  $z(t)$ .

This yields the equation:

$$\cos(\phi - wt) = \tan \theta \cot \Theta \quad (3.22)$$

The condition on the range of phi leads to a condition on when can we expect to have a source light up at its own location on the dirty map.  $-\cot \theta \leq \cot \Theta \leq \cot \theta$ .

As it turns out, this happens only when the absolute value of the source's latitude is less than the cone angle  $\Theta$ .

The SPA of the beam pattern matrix is;

$$B(\hat{\Omega}(t), \hat{\Omega}_o) = \Lambda(\hat{\Omega}(t))\Gamma(\hat{\Omega}(t), t)\Gamma(\hat{\Omega}_o, t) \frac{\sqrt{f_u} - \sqrt{f_l}}{w} \sqrt{\frac{8c}{[\hat{\mathbf{z}} \cdot \Delta \mathbf{r}(t)][\hat{\mathbf{z}} \cdot (\hat{\Omega}(t) - \hat{\Omega}_o)]}} \quad (3.23)$$

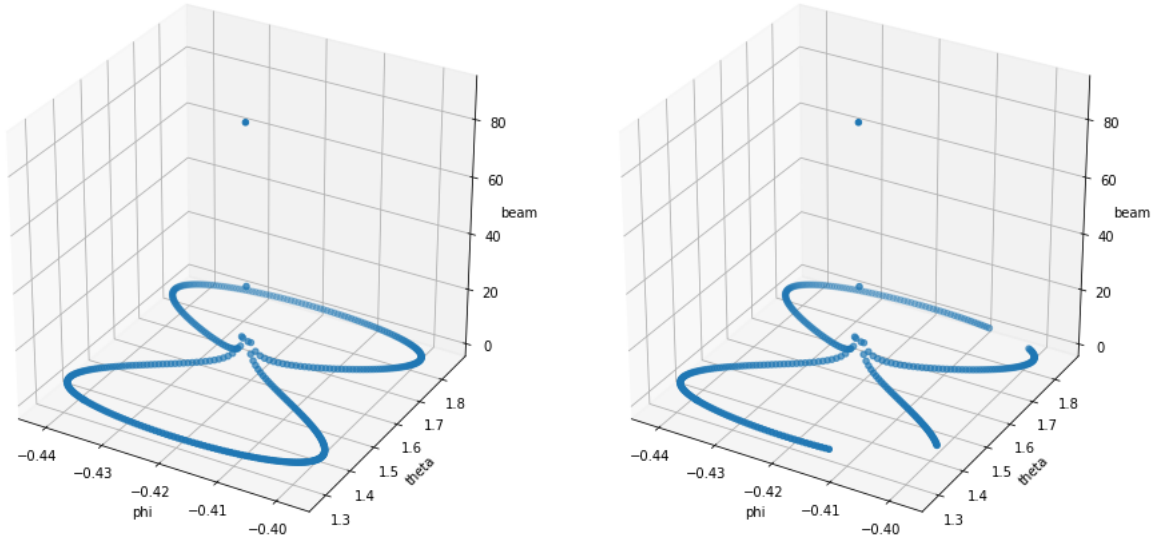
Since there is a denominator term, the first obvious thing to look for is the condition when the denominator goes to zero, for then the SPA is not applicable.

As it turns out this condition is when  $\hat{\mathbf{z}} \cdot \Delta \mathbf{r}(t) = 0$  i.e. the two detectors are on the same latitude.

### 3.4 Power Distribution

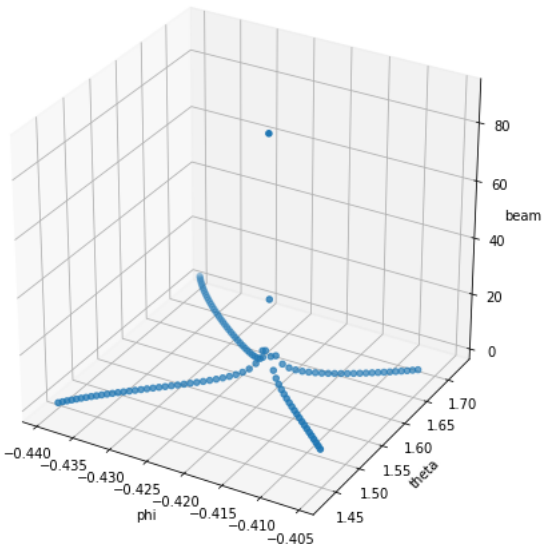
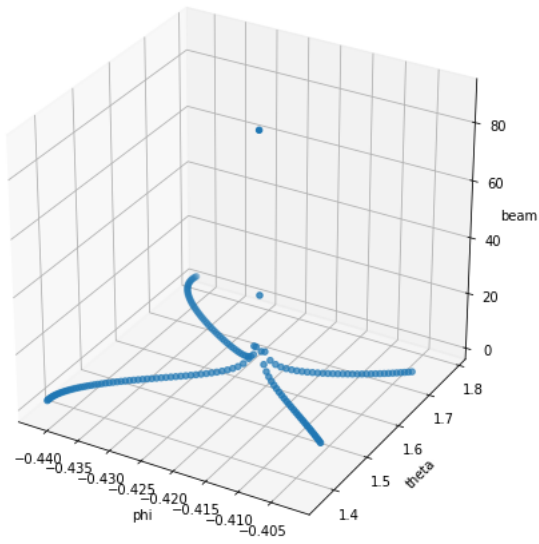
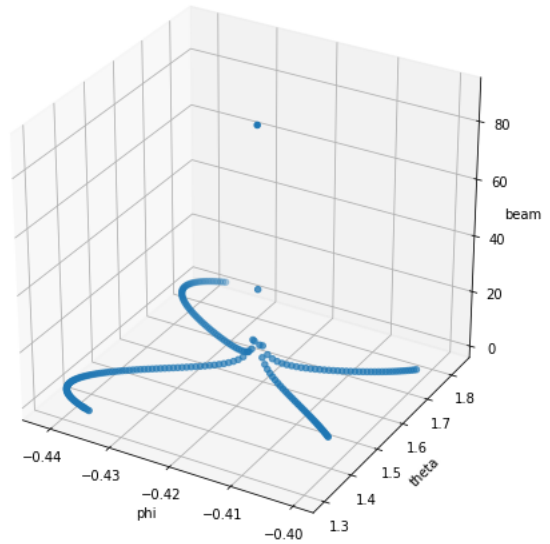
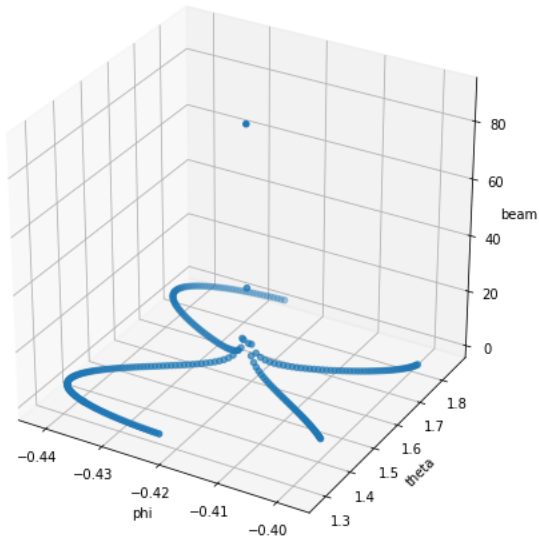
One of the first things to look for in case of a point spread is the power distribution, for if there is a concentration of power in certain regions of the curve, the curve can be approximated by those regions of concentrated power.

The graphs below show the fractional power concentration for a source at the equator. From left to right the fractional power goes from 100 percent to 50 percent. The source is at the origin.



Note that for a source with  $-\Theta \leq \theta \leq \Theta$ , the power peaks at the source location. In fact the curve is singular at this point. The power however is not concentrated in a particular region which forces us to consider the entire curve in our analysis





# Chapter 4

## Groebner Basis and Stereographic Projection

### 4.1 Basics of Algebraic Geometry

As mentioned before that the point spread functions intersect each other, it was of interest to study these intersections. The first method that was employed to study these intersections was one of Algebraic Geometry. The reason why this method was pursued is because Algebraic Geometry enables us to translate an algebraic problem involving polynomial equations to a problem on vectors spaces, the solution set of the algebraic problem and vice-versa.

#### Ideals

Consider a set  $F$  of  $m$  polynomials in  $n$  variables  $(x_1, x_2, \dots, x_n)$  such that  $F = \{f_1, f_2, \dots, f_m\}$ . The space of functions that can be represented as a linear combination of the elements of  $F$  is called the ideal of  $F$  and denoted by  $I(F)$ . This implies given some arbitrary function  $g(\mathbf{X}) \in I(F)$ ;

$$g(\mathbf{X}) = \sum_i c_i(X) f_i(X) \tag{4.1}$$

The important thing to remember here is that we are not working with a vector space and there is no reason to assume that the linear combinations are unique.

## Varieties

Given an ideal  $I$ , the set of solutions of  $I$  is called the variety of  $I$  and denoted by  $V(I)$ . If  $a = \{a_1, a_2, \dots, a_n\}$  is an arbitrary element of  $V(I)$  then, for all  $f \in I$   $f(a) = 0$ .

If  $I$  is an ideal of  $F$  such that  $I = (f_1, f_2, \dots, f_m)$  and  $V_i$  denotes the variety of  $f_i$  then,

$$V(I) = \bigcap_{i=1}^m V_i \quad (4.2)$$

An intuitive proof for the above equation goes something like this;

If  $g$  is an arbitrary element of  $I$ , then by the definition of an ideal,  $g = \sum_{i=1}^m c_i f_i$ . Let  $\mathbf{x}_i$  denote an arbitrary element of  $V_i$ . Then  $\mathbf{x}_i \in V(g)$  iff  $\mathbf{x}_i \in V_j$  for all  $j \in \{1, \dots, m\}$ . Hence;

$$V(g) = \bigcap_{i=1}^m V_i \quad (4.3)$$

Since  $g$  is arbitrary element of  $I$ , condition (4.3) is valid for all  $g \in I$ . Hence, the validity of equation (4.2) is established.

## Ordering

Ordering of variables in algebraic geometry is defining the prominence of the variables. What is meant by it is that if there are two variables  $x_1$  and  $x_2$  such that  $x_1$  is more prominent than  $x_2$  which can be represented as  $x_1 > x_2$  then for two monomials  $x_1^m x_2^n$  and  $x_1^k x_2^l$   $x_1^m x_2^n > x_1^k x_2^l$  if  $m > k$  irrespective of the relation between  $n$  and  $l$ . The ordering is not unique and depends on the user's choice. In the case of polynomials in  $n$  variables  $(x_1, x_2, \dots, x_n)$  the ordering can be such that  $x_1 > x_2 > \dots > x_n$ . This particular ordering is called lexical ordering.

## Least Common Multiple(LCM)

Let  $f$  and  $g$  be two monomials in  $n$  variables in  $(x_1, x_2, \dots, x_n)$  such that  $f = x_1^{l_1} x_2^{l_2} \dots x_n^{l_n}$  and  $g = x_1^{k_1} x_2^{k_2} \dots x_n^{k_n}$  where  $l_i$  and  $k_i$  are all positive integers.

If  $M_i = \max(l_i, k_i)$  denotes the maxima between  $l_i$  and  $k_i$  then,

$$LCM(f, g) = \prod_{i=1}^n x_i^{M_i} \quad (4.4)$$

$\text{LCM}(f,g)$  is divisible by both  $f$  and  $g$ . This fact is evident from its definition.

## S polynomial

Consider the set  $F$  of  $m$  polynomials in  $n$  variables  $(x_1, x_2, \dots, x_n)$  whose  $i^{\text{th}}$  element is given by  $f_i$ , with a defined ordering say  $x_1 > x_2 > \dots > x_n$ . Let  $LT(f_i)$  denote the leading term in the polynomial  $f_i$  which is the one with the highest power of  $x_1$  and if  $f_i$  is independent of  $x_1$  then the term with leading power of  $x_2$  and so on. Let  $LC(f_i)$  define the corresponding leading coefficient and  $LM(f_i)$  the corresponding leading monomial.

Then the S polynomial of  $f_i f_j$  is defined as;

$$S(f_i, f_j) = \frac{\text{LCM}(LT(f_i), LT(f_j))}{LC(f_i)LT(f_i)} f_i - \frac{\text{LCM}(LT(f_i), LT(f_j))}{LC(f_j)LT(f_j)} f_j \quad (4.5)$$

Notice that  $S(f_i, f_i) = 0$ .

## Groebner Basis

Given an ideal  $I$ , the Groebner basis of  $I$  is the generator set  $G$  of  $I$  i.e. any element of  $I$  can be represented as a linear combination of the elements of the  $G$ .

Considering two polynomials  $f_1$  and  $f_2$  of  $n$  variables  $(x_1, x_2, \dots, x_n)$  with the lexical ordering  $x_1 > x_2 > \dots > x_n$ . If  $f_1 > f_2$  based on the lexical ordering used here, then  $f_1$  can be written as  $f_1 = c_1 f_2 + r_1$ , where  $r_1 < f_2$  and  $c_1$  and  $r_1$  are polynomials of the  $n$  variables  $(x_1, x_2, \dots, x_n)$ . Using equation (3.3);  $V(f_1) = V(f_2) \cap V(r_1)$ .

Now since  $r_1 < f_2$ , the above procedure is repeated and we obtain  $f_2 = c_2 r_1 + r_2$  where,  $r_2 < r_1$  and  $V(f_1) = V(f_2) \cap V(r_1)$ . This process is repeated until the condition  $r_{i-1} = c_{i+1} r_i$  for some  $i$  is reached. The Groebner basis for the ideal  $I(f_1, f_2)$  is now defined by the set  $G = \{f_1, f_2, r_1, \dots, r_i\}$ .

The procedure can be extended to a system of any  $m$  number of polynomials. Though it becomes increasingly cumbersome. In order to calculate the Groebner basis there exists one of the most well known algorithms in Algebraic Geometry called Buchberger's Algorithm.

A feature that makes Groebner basis interesting is that the variables that are given the highest prominence are the first to be removed from subsequent Groebner bases. A polynomial in  $n$  variables  $(x_1, x_2, \dots, x_n)$  where the variables belong to a  $\mathbf{K}$  vector space basically defines a surface in the said  $\mathbf{K}$  space. If  $f$  and  $g$  are two such polynomials in this  $\mathbf{K}$  space then their intersection defines a hypersurface in  $\mathbf{K}$ . An  $m$ -dimensional hypersurface in an  $n$  dimensional vector space requires only  $m$  independent variables. The remaining  $n-m$  variables can be determined using the equation of the hypersurface. The vanishing of highest order variables in the calculation of Groebner basis captures exactly this feature.

### Buchberger's Algorithm

Consider the set  $F$  of  $m$  polynomials and the corresponding ideal  $I(F)$ . Setting  $G = F$

$$G' = G$$

Denote the number of elements in  $G$  by  $num$

Denoting the  $i^{th}$  element of  $G$  by  $g_i$

Calculate the S-polynomial  $S(g_i, g_j)$ .

Divide  $S(g_i, g_j)$  by the elements of  $G$  i.e. express it in the form  $S(g_i, g_j) = \sum_{i=1}^{num} g_i + r_{ij}$  where  $r_{ij}$  is the remainder.

If  $r_{ij} \neq 0$ , then  $G = G \cup \{r_{ij}\}$

If  $G' \neq G$ , continue in the loop.

If  $G' = G$ , end the loop

$G'$  thus obtained is the required Groebner basis.

*(Check reference [2] for proof)*

There is also a modified Buchberger's algorithm to reduce the number of steps taken to construct the Groebner Basis for a given ideal though it runs on the same basic principle. Buchberger's algorithm is instrumental for any computational algebraic geometry problem.

## 4.2 Groebner Basis for Point Spread Function

The motive behind the use of the Groebner Basis is given by the property of the Varieties, if  $f$  is a polynomial which is given as a linear combination of polynomials  $\{g_1, g_2, \dots, g_n\}$ , then the set of solutions of  $f$  is given by the intersection of the solution sets of the  $g_i$ s.

The aim is to look for something akin to a superstructure for the entire point spread function. Superstructures often provide deeper insight into the problem. For the shape of the PSF these structures are the unit sphere and the cone formed by the rotating baseline. We as of yet do not have such a description for the the entire PSF i.e. the shape and the value at each point on the shape. The method of Groebner basis therefore facilitates in getting the solution of an equation of many variables by instead making us solve multiple equations but each in a lower number of variables, though with a higher order in the variables. The trade-off is that the equations become increasingly more complicated

In order to get the Groebner basis for the PSF we must first move from trigonometric equations to algebraic equations since the latter is easier to solve. We will proceed only with the shape of the PSF to gauge the difficulty in arriving at a generalized solution. In order to do that, denote  $\cos wt = u_t$  and  $\sin wt = v_t$  and they are related by the polynomial equation  $u^2 + v^2 - 1 = 0$ . Similarly denote variables for  $\cos \theta = u_\theta, \sin \theta = v_\theta, \cos \phi = u_\phi$  and  $\sin \phi = v_\phi$ .  $\Theta$  is a constant and is kept as it is.

Thus at the end we have 6 polynomials in 9 variables, namely  $(x, y, z, u_t, v_t, u_\theta, v_\theta, u_\phi, v_\phi)$ .

The 6 polynomial equations are:

$$x - v_\theta u_\phi + 2 \cos \Theta^2 v_\theta (u_\theta u_\phi + v_\theta v_\phi) u_t - \sin 2\Theta u_\theta u_t = 0 \quad (4.6)$$

$$y - v_\theta v_\phi + 2 \cos \Theta^2 v_\theta (u_\theta u_\phi + v_\theta v_\phi) v_t - \sin 2\Theta u_\theta v_t = 0 \quad (4.7)$$

$$z - \cos 2\Theta u_\theta - \sin 2\Theta (u_\theta u_\phi + v_\theta v_\phi) = 0 \quad (4.8)$$

$$u_t^2 + v_t^2 - 1 = 0 \quad (4.9)$$

$$u_\theta^2 + v_\theta^2 - 1 = 0 \quad (4.10)$$

$$u_\phi^2 + v_\phi^2 - 1 = 0 \quad (4.11)$$

Now the Groebner basis is calculated using the inbuilt Buchberger’s algorithm in python. The basis though comes out to be constituted of polynomials with order as high as 144 in the variable  $z$ . Note that which variable it is depends on the ordering set by the user. In this case the ordering was set to be  $(u_t > v_t > u_\phi > v_\phi > u_\theta > v_\theta > x > y > z)$ . The time dependent variables were given highest prominence in order to get rid of them much earlier in the Groebner basis calculation. As discussed before the trade-off for getting rid of variables is the increased complexity in the known variables. A thing to keep in mind that the source locations were also treated as variables.

A glance at the Stationary Phase Approximation of the beam pattern approximation reveals that there is a square root in the formula which needs to be done away with and hence, we will have to work with the square of the matrix element which upon closer inspection of the formula gives a polynomial equation of order 16 in  $u_t$  and  $v_t$ .

Since the Groebner basis increase in complexity with the number of polynomials and the complexity of the initial polynomials themselves, pursuing this brute force derivation will make the problem intractable and hence this approach hasn’t been followed further.

### 4.3 Stereographic Projection

The stereographic projection is the projection of a 3-dimensional object onto a 2-dimensional surface. This particular method was chosen for two different reasons. The first was that when working with the stereographic projection we are working with polynomials instead of trigonometric functions for the former is easier to deal with. The second reason is that this particular formalism of the problem does away with the time dependence as will be seen later in the section.

Its important to remember that the time dependence in the PSF came from the stationary phase approximation but the dirty map that is numerically generated and what we have to work with does not explicitly carry any information about the time the particular pixel was lit up.

The projection will be taken on the  $xy$  plane. In order to calculate the stereographic projection first a reference point is chosen. Since this reference point will be mapped to

infinity on the xy plane, it is better to choose as reference a point on the pole. Note that the analysis we have built this thesis on does not work for a source at either of the poles since the statistic is constructed based on the fact that the angle between the baseline vector and the unit vector  $\hat{\Omega}$  changes as the Earth rotates which is not the case when the source is at the pole for then the angle is  $\Theta$ (the cone angle) which is constant.

The point (0,0,1) is defined as the reference point O. For an arbitrary point P=(x,y,z) on the unit sphere a line is drawn connecting P and O. The point where this line intersects the xy plane is the stereographic projection of point P and is denoted by Q.

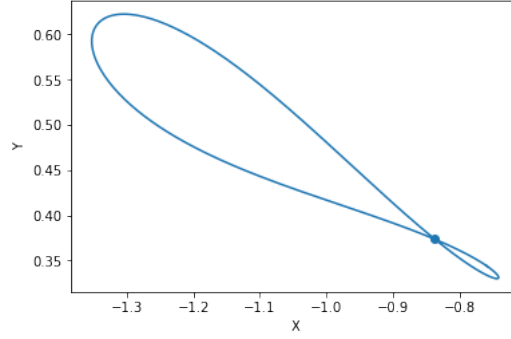
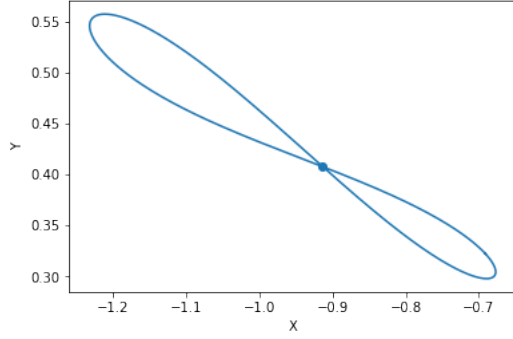
Let Q=(X,Y,0), then using the fact that P,Q and O all lie on the same line;

$$\frac{x}{X} = \frac{y}{Y} = \frac{z-1}{-1} \quad (4.12)$$

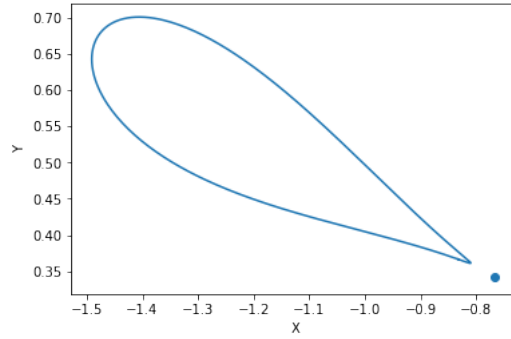
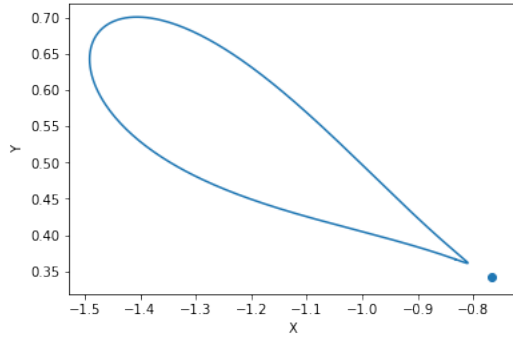
which combined with the equation for a unit sphere  $x^2 + y^2 + z^2 = 1$  gives:

$$X = \frac{x}{1+z}; Y = \frac{y}{1+z} \quad (4.13)$$





from left to right  $\theta = 0^\circ$  and  $\theta = 5^\circ$



from left to right  $\theta = 10^\circ$  and  $\theta = 15^\circ$

The figures above are the stereographic projections for sources at  $\phi = 150^\circ$  with varying  $\theta$ . The dots represent the source location

Since the stereographic projections also carry a rotational symmetry,  $\phi$  can be set to zero without any loss of generality.

Lets start with the simple case when the source is at the equator i.e.  $\theta = \frac{\pi}{2}$ . For such a source;

$$X = \frac{1 - 2 \cos \Theta^2 \cos wt^2}{1 + \sin 2\Theta \cos wt} \quad (4.14)$$

$$Y = \frac{-2 \cos \Theta^2 \cos wt^2}{1 + \sin 2\Theta \cos wt} \quad (4.15)$$

The above equations can now be written as quadratic equations in  $\cos wt$ .

The two quadratic equations that are obtained are;

$$A \cos^2 wt + B \cos wt + C = 0 \quad (4.16)$$

$$A' \cos^2 wt + B' \cos wt + C' = 0 \quad (4.17)$$

where the coefficients A,B and C are given by;

$$A = 2 \cos^2 \Theta, B = -X \sin 2\Theta, C = X - 1 \quad (4.18)$$

The coefficients A', B' and C' are a bit more involved and given by;

$$A' = R^2 \sin^2 2\Theta \quad (4.19)$$

$$B' = -2(R^2 \sin 2\Theta - X \sin 2\Theta \sin^2 \Theta) \quad (4.20)$$

$$C' = R^2 - 2X \sin^2 \Theta - \cos 2\Theta \quad (4.21)$$

where  $R^2 = X^2 + Y^2$ .

The time dependence is now removed by using the formula;

$$\frac{\cos^2 wt}{BC' - B'C} = \frac{\cos wt}{CA' - C'A} = \frac{1}{AB' - A'B} \quad (4.22)$$

This removal of time dependence leads to the following equations;

$$(R^2 + 1)(R^2 - 2X + 1) \cos 2\Theta + R^2(X - 2) + X = 0 \quad (4.23)$$

Now that we have obtained the corresponding algebraic equation for the stereographic projection of the shape of the point spread for a source at the equator, we calculate the same for a general for a source at any arbitrary latitude  $\theta$ .

$$X = \frac{\sin \theta - 2 \cos^2 \Theta \sin \theta \cos^2 wt + \sin 2\Theta \cos \theta \cos wt}{1 - \cos 2\Theta \cos \theta - \sin 2\Theta \sin \theta \cos wt} \quad (4.24)$$

$$X = \frac{-2 \cos^2 \Theta \sin \theta \cos wt \sin wt + \sin 2\Theta \cos \theta \sin wt}{1 - \cos 2\Theta \cos \theta - \sin 2\Theta \sin \theta \cos wt} \quad (4.25)$$

After some algebra two equations quadratic in  $\cos wt$  are obtained.

$$A \cos wt^2 + B \cos wt + C = 0 \quad (4.26)$$

$$A' \cos wt^2 + B' \cos wt + C' = 0 \quad (4.27)$$

The coefficients A,B and C are given by:

$$A = 2 \cos^2 \Theta \sin \theta \quad (4.28)$$

$$B = -2 \sin \Theta (X \sin \theta + \cos \theta) \quad (4.29)$$

$$C = (1 - \cos 2\Theta \cos \theta)X - \sin \theta \quad (4.30)$$

The coefficients A',B' and C' are given in terms of A, B, C and three auxilliary functions a, b and c where,

$$a = 1 - \cos 2\Theta \cos \theta \quad (4.31)$$

$$b = \sin 2\Theta \sin \theta \quad (4.32)$$

$$c = \sin 2\Theta \cos \theta \quad (4.33)$$

The primed coefficients are now given by:

$$A' = A(b^2 + Y^2 + B(2 + c)) \quad (4.34)$$

$$B' = A(A + c)(2c + B) - Bc^2 + ABC - 2abAY^2 \quad (4.35)$$

$$C' = a^2AY^2 - (A + C)(c^2 - AC) \quad (4.36)$$

The time dependence can now be removed. It is to be noted that the time dependence arrived after the stationary phase approximation. The reason for is that for a given image point on the dirty map, the contribution from a source location say  $\widehat{\Omega}_o$  occurs at all times but because there is also a sum over frequency, the contributions cancel unless the conditions for the stationary phase occur at which point there is a signal peak. This of course occurs at a particular time and hence the time dependence. Since the output signal  $S(\widehat{\Omega})$  is time independent, it is imperative that any basis we arrive upon must be time independent.

The equation obtained after removing time dependence from the above equations is a quartic equation:

$$R^4 - 6R^2 + 1 + (R^2 + 1)^2(2 \cos 2\Theta + 2 \cos^2 \theta) - (R^4 - 1)(\cos(\theta - 2\Theta) + 2 \cos \theta + \cos(\theta + 2\Theta)) - 2(X \cos \phi + Y \sin \phi)(R^2 + 1)(\sin(\theta - 2\Theta) - 2 \sin \theta + \sin(\theta + 2\Theta)) = 0 \quad (4.37)$$

This quartic polynomial equation is completely parametrized by  $\theta$  in the sense that upon being plotted the shape of the projection completely depends upon  $\theta$ . As discussed before  $\phi$  leads to a rigid rotation around the origin with the z-axis as the axis of rotation. Being a quartic equation, two projections for different  $\theta$  have at most 4 points of intersection. Its a property that will be used in the later section to propose an approximate basis for the beam pattern matrix.

Efforts have been made to use these equations to get the basis but they haven't provided any additional information about the point spread. A thing of importance is that the point spread for two sources at the same longitude but latitudes  $\theta$  and  $-\theta$  have the same spread albeit rotated rigidly along an axis that crosses the origin and intersects the line joining the two sources perpendicularly. Though when a stereographic projection is taken, owing to the choice of a reference point, this symmetry is broken.

# Chapter 5

## Singular Value Decomposition

In the previous sections the shape of the point spread function was used in order to obtain a viable basis. If a basis using only the shape could be obtained, the analysis would be much more simple because the SPA value of the beam matrix is quite complicated to deal with. But as it turns out, the amount of information in the shape is not enough to determine it.

Singular value decomposition is the generalization of eigenvalue decomposition. Consider an  $m \times n$  beam pattern matrix  $\mathbf{M}$ . The matrix is then decomposed into 3 matrices  $\mathbf{U}$ ,  $\Sigma$ ,  $\mathbf{V}$  such that  $\mathbf{M} = \mathbf{U} \Sigma \mathbf{V}^T$ . The matrices  $\mathbf{U}$  and  $\mathbf{V}$  are  $m \times m$  and  $n \times n$  unitary matrices respectively i.e.  $\mathbf{U}^* \mathbf{U} = I_{m \times m}$  and  $\mathbf{V}^* \mathbf{V} = I_{n \times n}$  and  $\Sigma$  is a  $m \times n$  diagonal matrix.

Consider the  $m \times n$  matrix  $\mathbf{M}$ .  $\mathbf{M}$  is a map from an  $n$  dimensional vector space  $\mathbf{K}_n$  to an  $m$  dimensional vector space  $\mathbf{K}_m$ . Lets consider the action of  $\mathbf{M}$  on an arbitrary basis  $\mathbf{v}_1, \mathbf{v}_2, \dots, \mathbf{v}_n$  of the  $n$  dimensional vector space. Since the matrices  $\mathbf{U}_{m \times m}$  and  $\mathbf{V}_{n \times n}$  are unitary, there action on a vector is akin to a rotation. The action of the diagonal matrix  $\Sigma$  is to scale the axes. Thus the action of  $\mathbf{M}$  takes place in three steps.

First there is a rotation of the bases by  $\mathbf{V}^*$ , which is then followed by the scaling of the axes by the matrix  $\Sigma$ . After this another rotation is initiated by  $\mathbf{U}$ . If  $m < n$ , the operation of  $\Sigma$  scales  $n-m$  of the axes to zero. Now in order to do a numerical analysis it is better to oversample the space since it improves the signal to noise ratio. So if  $n_o$  is the number of pixels the detector pairs sample, the numerical analysis to get the  $S(\hat{\Omega})$  is done for an  $n > n_o$ . Thus implicitly, the beam pattern matrix takes as input the  $n$  P( $\hat{\Omega}$ ) and returns  $n$

$S(\widehat{\Omega})$  out of which only  $n_o$  are prominent. Thus upon taking the SVD of the beam pattern matrix, the diagonal matrix  $\Sigma$  has only  $n_o$  prominent diagonal values. Since the singular values are calculated such that in the matrix  $\Sigma$ , they occur in the order from highest to lowest, upon being plotted one must observe a fall in the singular values after  $n_o$ .

Using the SVD on the beam pattern matrix  $\mathbf{B} = \mathbf{U} \Sigma \mathbf{V}^T$ . Using the unitarity of  $\mathbf{U}$ ;  $\mathbf{B}^T \mathbf{B} = \mathbf{V} \Sigma \Sigma \mathbf{V}^T$ . Since  $\mathbf{B}$  is a real and symmetric matrix, therefore  $\mathbf{B}^2 = \mathbf{V} \Sigma \Sigma \mathbf{V}^T$ .

Consider the matrix  $\mathbf{V}$ . The  $i^{th}$  column of  $\mathbf{V}$  is the singular vector corresponding to the  $i^{th}$  singular value.

Since  $\mathbf{B}$  is symmetric therefore,  $\mathbf{V} \Sigma \mathbf{V}^T$ . If the  $i^{th}$  singular vector is given by  $v_i$ , the  $i^{th}$  singular value denoted by  $\sigma_i$  ( $\sigma_i = \Sigma_{ii}$ ) and the  $j^{th}$  element of this vector is denoted by  $[v_i]_j$  then,

$$\mathbf{B}_{ij} = \sum_{k=1}^n [v_k]_i \sigma_k [v_k]_j \quad (5.1)$$

Since the singular values fall off after  $n_o$  therefore, the above equation can be rewritten as

$$\mathbf{B}_{ij} \simeq \sum_{k=1}^{n_o} [v_k]_i \sigma_k [v_k]_j \quad (5.2)$$

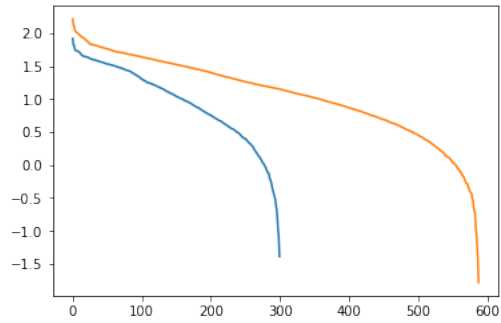
The singular values and singular vectors have been calculated for a toy problem with the LIGO detectors but the distance between them is halved to 1500 km bringing  $n_o$  to 300.

The calculation has been done for 2 different sample space. One with 300 pixels and the other with 568 pixels.

The plot below is for the singular values to discern their falloff point. The plot is logarithmic with base 10. The y-axis carries the log of the singular value and the x-axis simply marks the index of the singular value.

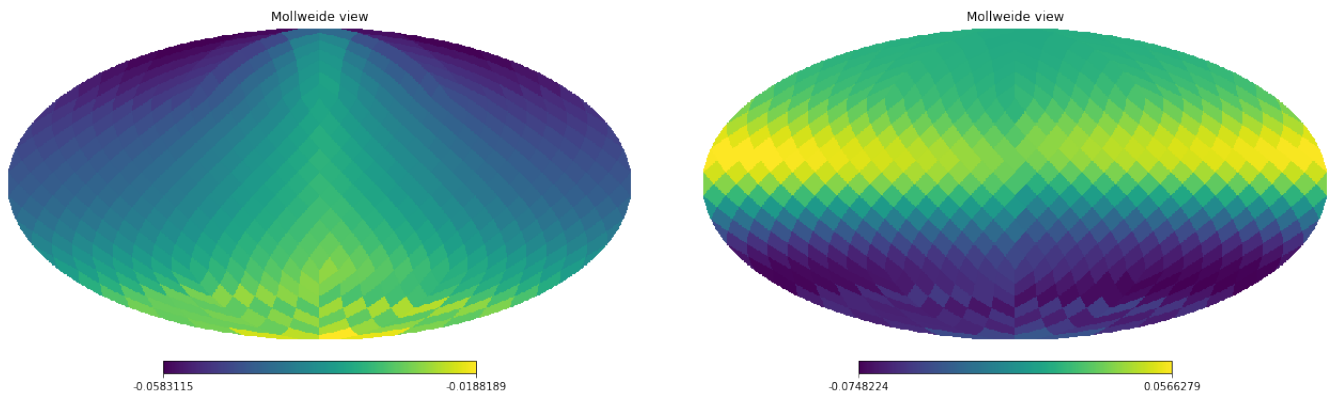
The singular values fall rapidly for the first few terms after which there is a long plateau where the fall off is gradual followed by another sudden fall off. It is interesting to note that only the first few singular vectors corresponding to the initial few highest singular values have any discernible pattern. The rest of the singular vectors upon being plotted appear completely random.

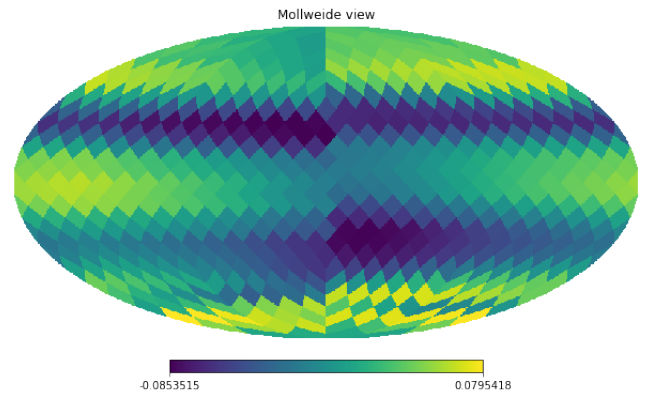
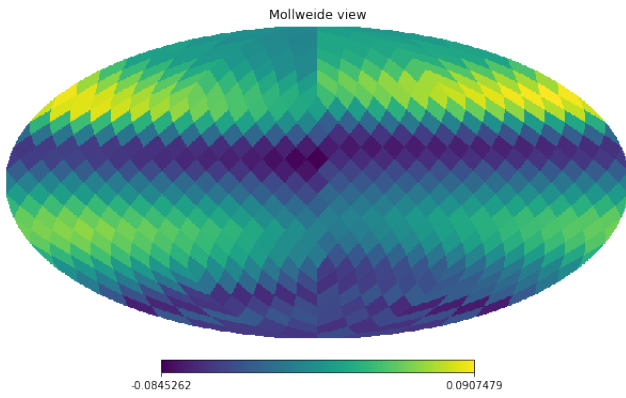
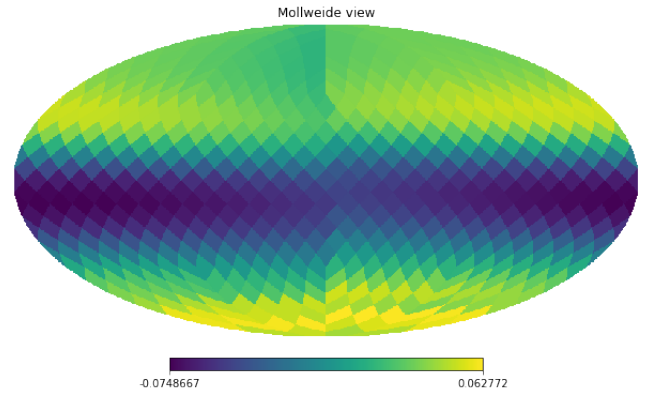
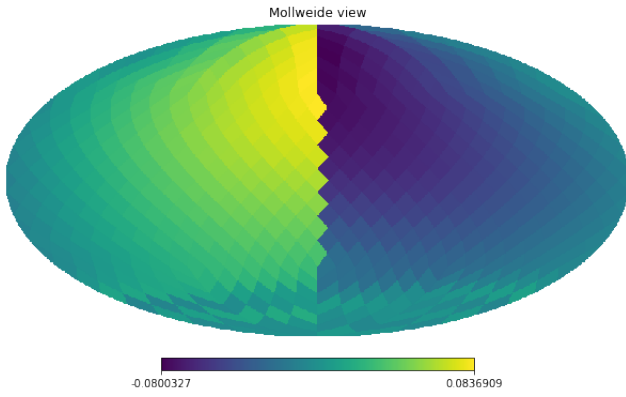
*The singular vectors are identified by the index of their corresponding singular values.*



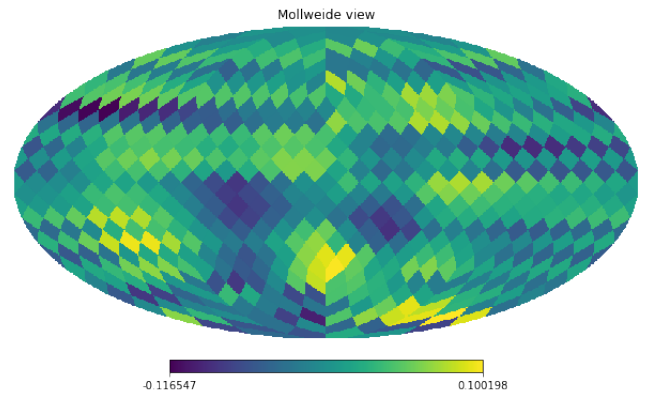
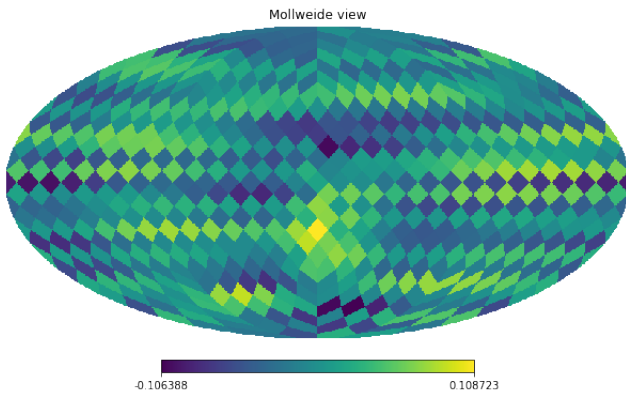
*singular value plot. Orange line is for 588 pixels and blue line is for 300 pixels*

The plot of the first 6 singular vectors for 588 pixels:

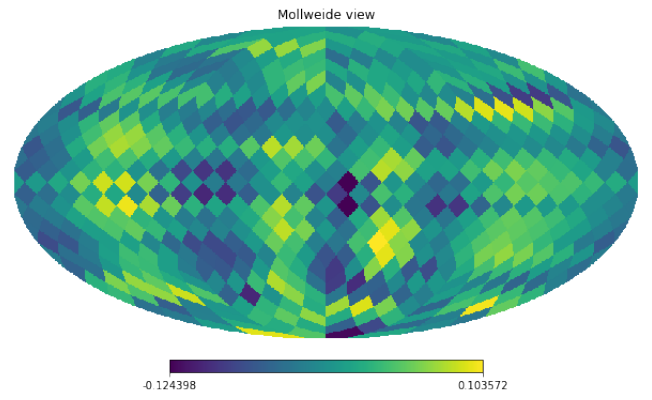
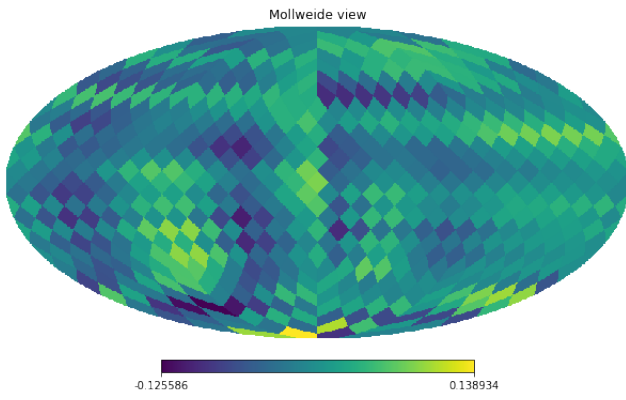
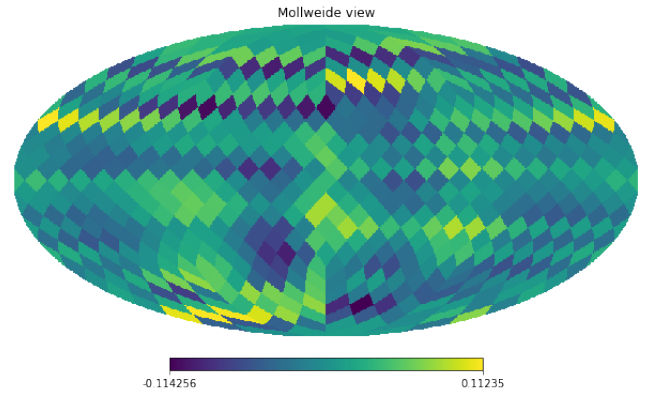
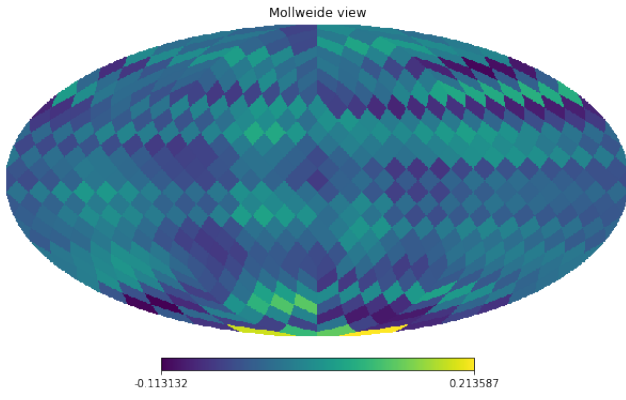




The plot of the 6 singular vectors from index 30 to 35 for 588 pixels:







## 5.1 Spherical Decomposition of Singular Vectors

Once the singular vectors are obtained, it needs to be checked whether it can be expanded in the form of simpler functions. The most obvious choice is the spherical harmonics.

Expanding the  $i^{th}$  singular vector into spherical harmonics:

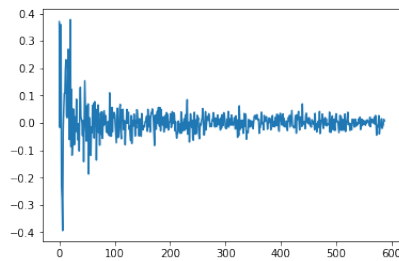
$$v_i(\theta, \phi) = \sum_{l,m} a_i^{lm} Y_{lm}(\theta, \phi) \quad (5.3)$$

The coefficients  $a_i^{lm}$  are given by:

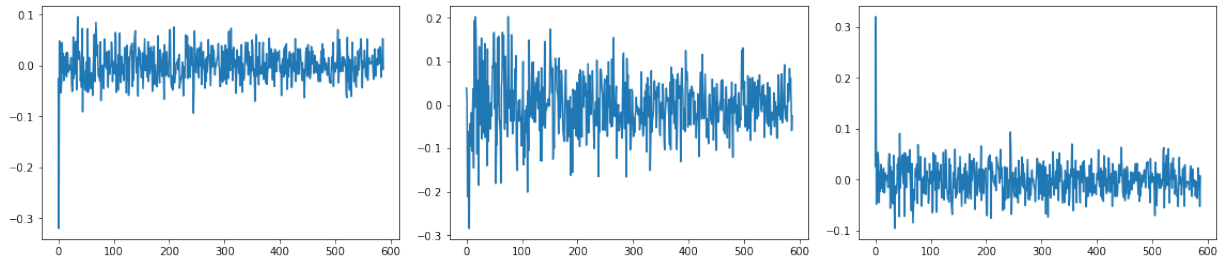
$$a_i^{lm} = \int_{S^2} v_i(\theta, \phi) Y_{lm}^*(\theta, \phi) \sin \theta \, d\Omega \quad (5.4)$$

The plots below show the coefficients from  $l=0$  to  $l=3$ . *The y-axis marks the coefficients and the x-axis marks index of the singular vector*

### 5.1.1 $l=0$

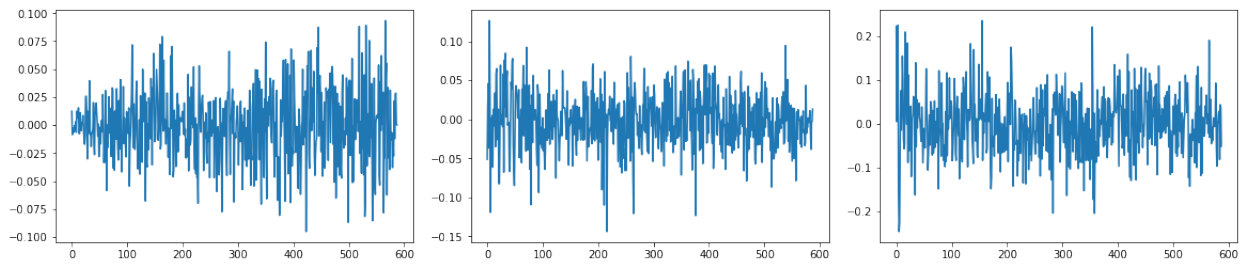


### 5.1.2 $l=1$

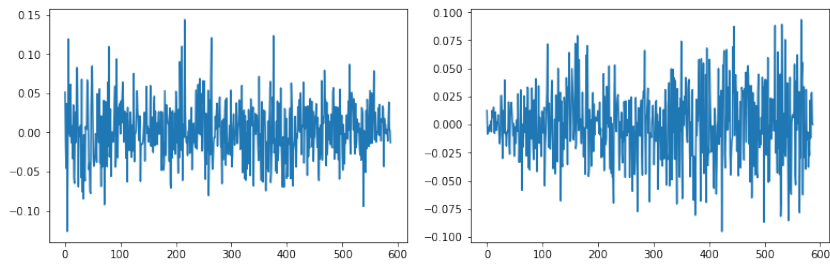


*from left to right  $m=-1$  to  $m=1$*

### 5.1.3 $l=2$

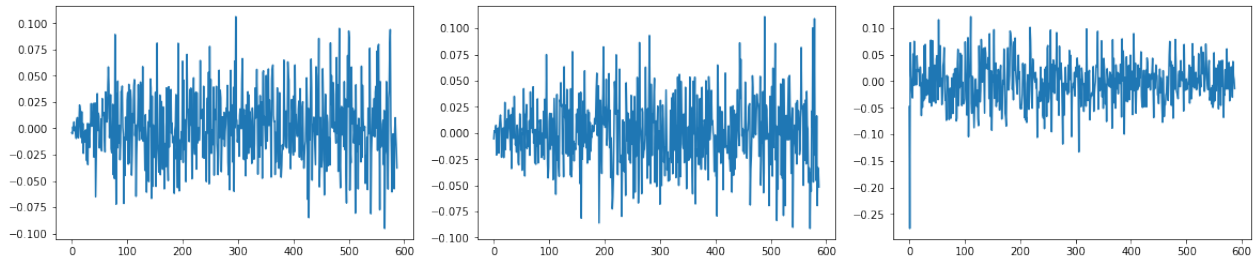


*from left to right  $m=-2$  to  $m=0$*

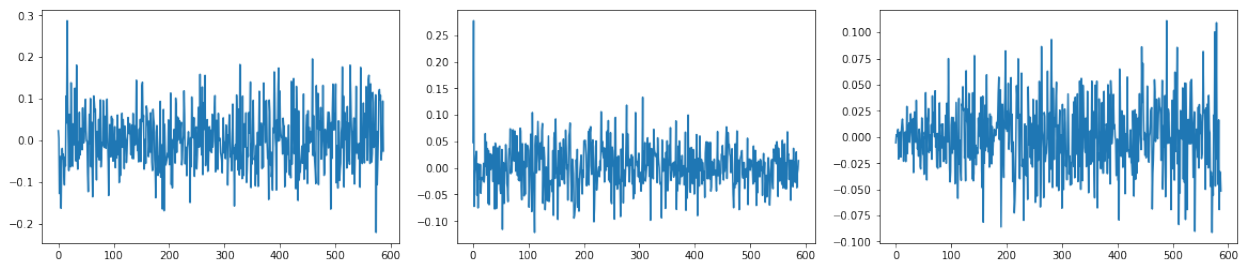


*from left to right  $m=1$  to  $m=2$*

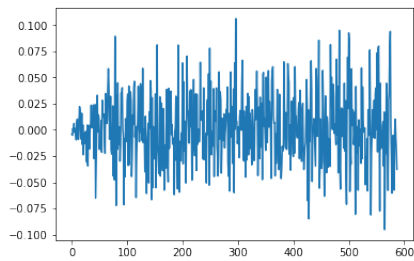
### 5.1.4 $l=3$



*from left to right  $m=-3$  to  $m=-1$*



*from left to right  $m=0$  to  $m=2$*



$m=3$

As is discernible from the plots, apart from the first few singular vectors, the rest of the vectors cannot be constructed from the spherical harmonics. This lack of any discernible pattern among the majority of the singular vectors makes it difficult to decompose them into any simple functions. However it still needs to be checked what is the relative error if the beam pattern matrix is reconstructed from the coefficients  $a_i^{lm}$ . For this particular analysis the coefficients were constructed till  $l = 20$ . Since  $-l \leq m \leq l$  therefore for a given  $l$  the number of spherical harmonics is  $2l+1$ . The total number of spherical harmonics calculated to reconstruct  $\mathbf{B}$  is then given by  $\sum_{l=0}^n (2l+1) = n^2 + 2n$  which for  $n=20$  is given by 420. Note that the number of prominent singular vectors is only around 300, so we are oversampling.

The relative error however turns out to be large, the same order of magnitude as the beam matrix itself. This approach has therefore been dropped.

A point to note is that we haven't been able to figure out the decomposition of the singular vectors into simple functions, it might be that this approach needs to be combined with efforts through other analytical approaches in order to help solve the problem. The usefulness of the SVD is therefore still an open question in this problem.

# Chapter 6

## An Approximate Basis

As discussed at the end of chapter 3, the quartic equations suggest that point spread curves for two different source locations at most intersect at 4 distinct places. This implies that if  $\mathbf{b}_i$  denotes the  $i^{th}$  column of the beam pattern matrix then,

$$\mathbf{b}_j^T \mathbf{b}_i \ll \mathbf{b}_i^T \mathbf{b}_i \quad (6.1)$$

Now lets consider the action of  $\mathbf{B}$  on  $\mathbf{b}_i^T$

$$\mathbf{b}_i^T \mathbf{B} = [\mathbf{b}_i^T \mathbf{b}_1, \dots, \mathbf{b}_i^T \mathbf{b}_{i-1}, \mathbf{b}_i^T \mathbf{b}_i, \mathbf{b}_i^T \mathbf{b}_{i+1}, \dots, \mathbf{b}_i^T \mathbf{b}_n] \quad (6.2)$$

which under the condition (5.1) becomes:

$$\mathbf{b}_i^T \mathbf{B} \simeq [0, \dots, 0, \mathbf{b}_i^T \mathbf{b}_i, 0, \dots, 0] \quad (6.3)$$

This implies that  $\mathbf{B}^T \mathbf{B}$  is an approximately diagonal matrix. An important thing to note is that the above calculation has been done considering the pixel size to be extremely small and the effect of noise has also been ignored.

Taking a note from the previous chapter the sky sphere is being oversampled. If the number of prominent singular vectors is  $n_o$  and the sky is divided into  $n$  pixels Then we have two sky maps,  $M_1$  with  $n_o$  pixels and  $M_2$  with  $n$  pixels then. A single pixel in  $M_1$  contains multiple pixels of  $M_2$ . The  $i^{th}$  column of  $\mathbf{B}$  given by  $b_i$  gives the spread for a source at the  $i^{th}$  pixel in the  $M_2$  map. Let  $S_i$  denote the set of pixels of  $M_2$  contained in the  $i^{th}$  pixel of

$M_1$ . The elements of  $S_i$  are now averaged and let this average vector be denoted by  $b_i^{ave}$ . The process is repeated for all pixels of  $M_1$ . The vectors thus obtained are used to construct a matrix  $\mathbf{B}_{ave}$ . Note that this is a  $n \times n_o$  matrix with the column given by the averaged vectors.

Taking the product  $\mathbf{B}_{ave}^T \mathbf{B}$ , the result is a  $n_o \times n$  matrix. Using equation (1.10),

$$\mathbf{B}_{ave}^T \mathbf{S} = \mathbf{B}_{ave}^T \mathbf{B} \mathbf{P} \quad (6.4)$$

The result is a  $n_o \times 1$  column vector. If  $n$  is large enough that the conditions (5.1) to (5.3) are valid then,  $\mathbf{B}_{ave}^T \mathbf{B}$  is a block diagonal matrix. Equation (5.4) gives a vector whose  $i^{th}$  element is dominated by power centred around a single direction in the sky sphere.

It still needs to be checked how well this method actually works numerically.

# Chapter 7

## Conclusion and Future Possibilities

Though progress has been made towards solving the problem, a viable basis has not been found. The last method that has been discussed if it turns out to be successful does not as such give us a basis. The problem for finding an analytical solution is much more difficult. During the course of the project a couple other methods were also tried. One of them was to decompose the point spread in fourier space and study it. The fourier series for the equations (3.4) to (3.6) is extremely simple and gives only around 22 independent components that depend upon  $(\theta, \phi)$ , though no further progress could be made from there on out. One possible reason for the difficulty in solving this problem is that the space we are working on is a quotient space as was described in the beginning of the thesis, which has been overcompleted by the point spread functions. By overcompleteness what is meant is that even upon removing the a few point spread functions, the rest will still cover the entire unit sphere. Quotient spaces on there own are difficult to work with.

It could be that an analytical solution to the problem might be possible when the value of the point spread function along with its shape is also taken into account. Though as discussed, even though the shape of the point spread function is quite easy to discern, the corresponding values are quite cumbersome to deal with. A major problem that is being encountered is the lack of a decomposition of the point spread functions into simpler functions.

A mathematical analysis that explicitly deals with overcomplete spaces might be useful in solving this problem. The mathematics of frame theory is one such analysis. The basic



idea is that one looks for an overcomplete basis for a proposed problem since the solving the problem involves the introduction of a generalization of bases that prioritizes span over linear independence. The basics of this subject have been studied during the course of this thesis, but as of right now no methodology has been discovered that can aid in the analysis. Though its usefulness is still open to debate. The prerogative for looking in this particular direction is that frame theory is being used extensively in signal analysis. It might be that the problem could be solved by involving multiple detectors but since the dirty map depends on the combination of detectors used it is not clear how if at all it could be done by this method. The problem is very much an open problem and if a general method to solve such a problem can be obtained it will prove instrumental in researches involving interferometric systems for spread functions in such systems is not that uncommon.

# Bibliography

- [1] S. Mitra, S. Dhurandhar, T. Souradeep, A. Lazzarini, V. Mandic, S. Bose and S. Balmer, Phys. Rev. D 77, 042002 (2008)
- [2] The plots shown above have been generated for detectors with the same location and orientation as LIGO Livingston and Hanford except in chapter 4. The plots obtained are dependent on the the detector location.
- [3] Cox, David A, Little, John, Oshea, Donal; *Ideals, Varieties and Algorithms: An Introduction to Computational Algebraic Geometry and Commutative Algebra*, Fourth Edition, Springer